AEDC-TR-75-131

Capt. Locke

CHARACTERISTICS OF THE HOLOGRAPHICALLY RECONSTRUCTED IMAGE OF A POINT SOURCE OF RADIATION

ARNOLD ENGINEERING DEVELOPMENT CENTER
AIR FORCE SYSTEMS COMMAND
ARNOLD AIR FORCE STATION, TENNESSEE 37389

December 1975

Final Report for Period July 1, 1974 – March 31, 1975

Prepared for

ARNOLD ENGINEERING DEVELOPMENT CENTER (DY)
AIR FORCE SYSTEMS COMMAND
ARNOLD AIR FORCE STATION, TENNESSEE 37389

NOTICES

APPROVAL STATEMENT

This technical report has been reviewed and is approved for publication.

FOR THE COMMANDER

Marshall K Kingery

MARSHALL K. KINGERY
Research and Development
Division
Directorate of Technology

Robert O Dietz

ROBERT O. DIETZ
Director of Technology

REPORT DOCUMENTATION PAGE		READ INSTRUCTIONS BEFORE COMPLETING FORM
1. REPORT NUMBER AEDC-TR-75-131	2. GOVT ACCESSION NO.	3. RECIPIENT'S CATALOG NUMBER
4. TITLE (and Subtitle) CHARACTERISTICS OF THE HOLOGRAPHICALLY RECONSTRUCTED IMAGE OF A POINT SOURCE OF RADIATION		5. TYPE OF REPORT & PERIOD COVERED Final Report - July 1, 1974 - March 31, 1975 6. PERFORMING ORG. REPORT NUMBER
7. AUTHOR(s) R. W. Menzel, ARO, Inc.		8. CONTRACT OR GRANT NUMBER(s)
9. PERFORMING ORGANIZATION NAME AND ADDRESS Arnold Engineering Development Center (DY) Air Force Systems Command Arnold Air Force Station, Tennessee 37388		10. PROGRAM ELEMENT, PROJECT, TASK AREA & WORK UNIT NUMBERS Program Element 65807F
11. CONTROLLING OFFICE NAME AND ADDRESS Arnold Engineering Development Center(DYFS) Air Force Systems Command Arnold Air Force Station, Tennessee 37388		12. REPORT DATE December 1975 13. NUMBER OF PAGES 16
14. MONITORING AGENCY NAME & ADDRESS(if different from Controlling Office)		15. SECURITY CLASS. (of this report) UNCLASSIFIED 15a. DECLASSIFICATION/DOWNGRADING SCHEDULE N/A

16. DISTRIBUTION STATEMENT (of this Report)

Approved for public release; distribution unlimited.

17. DISTRIBUTION STATEMENT (of the abstract entered in Block 20, if different from Report)

18. SUPPLEMENTARY NOTES

Available in DDC

19. KEY WORDS (Continue on reverse side if necessary and identify by block number)

holography
systems analysis
diffraction
focal characteristics

20. ABSTRACT (Continue on reverse side if necessary and identify by block number)

The focal volume characteristics of an image obtained from the recontruction of a hologram of a point source of radiation are described. The similarity between the reconstructed image and a point image obtained from a diffraction-limited lens is explained. The focal depth limitations of the reconstructed image are experimentally presented.

PREFACE

The work reported herein was conducted by the Arnold Engineering Development Center (AEDC), Air Force Systems Command (AFSC), under Program Element 65807F. The results were obtained by ARO, Inc. (a subsidiary of Sverdrup & Parcel and Associates, Inc.), contract operator of AEDC, AFSC, Arnold Air Force Station, Tennessee, under ARO Project Number B32S-04A. The author of the report was R. W. Menzel, ARO, Inc. The manuscript (ARO Control No. ARO-OMD-TR-75-89) was submitted for publication on June 23, 1975.

CONTENTS

ILLUSTRATION

1.0 INTRODUCTION

The usefulness of holography as a data-gathering tool is determined primarily by the accuracy with which data can be reconstructed from the hologram. A study of this problem can be approached by applying a linear systems analysis to the holographic process (Refs. 1 and 2).

By the principle of superposition for linear systems, the presence of any one excitation is not affected by the response attributable to other excitations. A complicated input function can be considered to be composed of multiple simpler functions, such as the components of a Taylor series or a Fourier spectrum, and the response of the system can be studied for each component. One such approach is to study the transform characteristics of the system to an impulse function input. The output caused by a complicated input is then the superpositioning integral (mathematically, the convolution) of the impulse transform function over the input function domain.

The optical analog of an impulse function is a point source of radiation. Invoking Huygen's principle, a radiating surface illuminance is the integration of a point source over the radiating area. By considering the transfer response of an optical system to a point radiating source, one can find the essential features of the resolution characteristics of the system.

Point sources of radiation are described in scalar diffraction theory by Green's function

$$G = A \frac{e^{ikr}}{r} \tag{1}$$

where A is the amplitude, $k = 2\pi/\lambda$, λ is the wavelength, and r is the distance between the point source and the point of observation (i.e., detection). The physical analog of Green's function is the $\overline{E}$ field obtained in the far field radiation zone of an electric dipole (Ref. 3):

$$\overline{E} = k^2 \frac{e^{ikr}}{r} (\hat{n} \times \overline{p}) \times \hat{n} \tag{2}$$

where $\bar{p}$ is the dipole moment and A is the unit vector. This further suggests that scalar diffraction theory should be restricted to the far field radiation zone requirements. In other words, the radiation wavelength should be small compared to the diffraction aperture which, in turn, should be small compared to the observation distance.

It is necessary to point out that the Green's function description is not adequate to describe plane wave radiation. Plane waves would, by Green's function, need to originate from a point infinitely distant from the observation point; this would reduce its amplitude to zero. A plane wave being characterized by its amplitude and phase front is adequately described by

$$G_p = Be^{i\Psi} \tag{3}$$

where the phase Ψ is defined relative to some plane perpendicular to the propagating direction along the radiation path.

By the Poynting theorem, the observed intensity is obtained from the product of the radiating field times its complex conjugate. By requiring that the intensities obtained from the plane wave and point source radiation have the same units, the units for A and B are, respectively, determined.

2.0 HOLOGRAPHIC RECORDING AND RECONSTRUCTION

The parameters for recording and reconstructing the hologram of a point source are defined in Fig. 1.

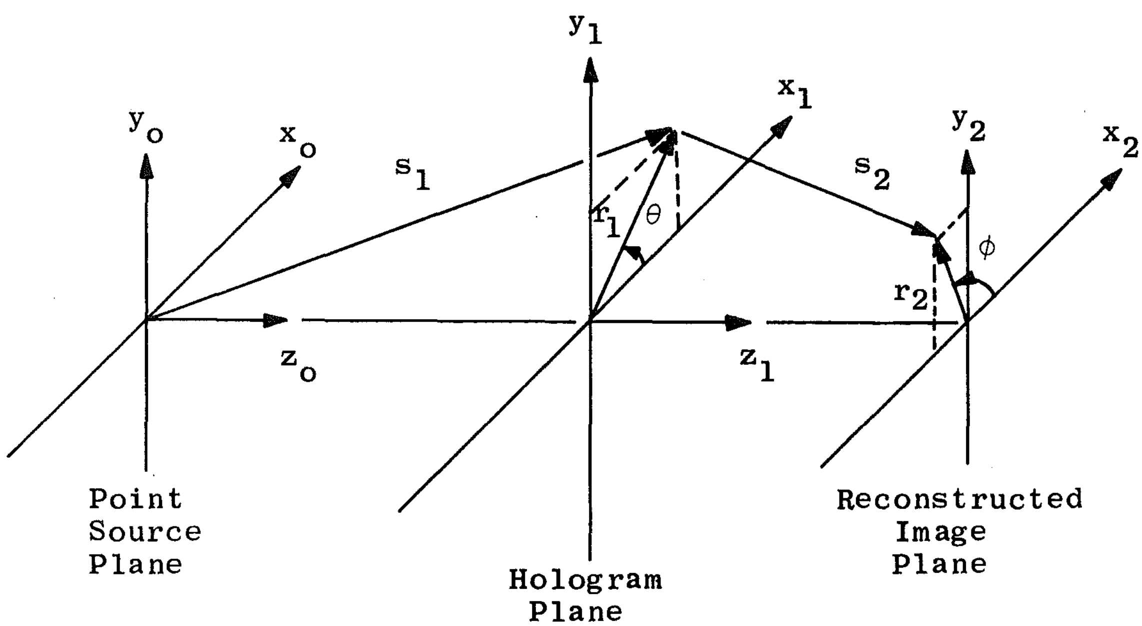

Figure 1. Definition of parameters.

The (x_i, y_i) with $i = 0, 1, 2$ are, respectively, the point source plane, the hologram recording plane, and the reconstructed image plane. Let λ_1 and λ_2 be the wavelength of the light in the recording and reconstruction mode, and let s_1 and s_2 be the distance between the point source plane and the hologram plane and the reconstructed image plane, respectively.

The recording is made by combining in the (x_1, y_1) plane light from the point source located at $(x_o = 0,\ y_o = 0)$ and plane waves propagating in the positive z-direction. After suitably developing the holographic film, the reconstruction is made by illuminating the hologram in the (x_1, y_1) plane by plane waves again propagating along the positive z-axis. All the optical axes have been made coincident for mathematical simplicity, not because of any inherent limitation in the holographic process.

Chosing the (x_o, y_o) plane for zero reference phase of the plane waves, then $\Psi = 0$ and the field U in the hologram plane will be

$$U = B + A \frac{e^{ik_1 s_1}}{s_1} \tag{4}$$

Restricting the field to a paraxial region, one can use the binominal expansion.

$$s_1 = (z_o^2 + r_1^2)^{1/2} = z_o + 1/2 \frac{r_1^2}{z_o} \tag{5}$$

where $r_1^2 = x_1^2 + y_1^2$. The assumption is made that higher order terms are small compared to λ_1 so that they contribute negligibly to the phase in U. The intensity in the hologram plane is obtained from the product of the field times its complex conjugate which gives

$$\begin{aligned} I &= B^2\left[1 + \frac{A^2}{z_o^2 B^2} + \frac{A}{z_o B} \cos\left(k_1\left(z_o + \frac{r_1^2}{2z_o}\right)\right)\right] \\ &= C_o + C_1 \cos\left(k_1\left(z_o + \frac{r_1^2}{2z_o}\right)\right) \end{aligned} \tag{6}$$

This result is similar to a Fresnel zone plate (Ref. 4). The circular symmetry about the z-axis is important in the reconstruction process.

The cosine term is the information carrying term; the C_o term contributes a constant bias term to the film exposure level which can generally be ignored in the reconstruction.

The reconstructed amplitude field $U_R(x_2, y_2)$ resulting from an illuminated hologram field $U_H(x_1, y_1)$ is

$$U_R = -\frac{i}{\lambda_2}\iint U_H \frac{e^{ik_2 s_2}}{s_2} \cos(\hat{n}, \bar{s}_2)\, dx_1 dy_1 \tag{7}$$

The field U_H is the product of an illuminating radiation source and the normalized hologram transmittance. When random phase shifts attributable to random film emulsion thicknesses can be neglected, the complex amplitude transmittance of the hologram is a linear mapping of the complex amplitude incident during exposure, provided the film exposure level is chosen properly (Ref. 2). Then for plane incident waves B' on the hologram,

$$U_H = B'\left[C_o' + C_1' \cos\left(k_1\left(z_o + \frac{r_1^2}{2z_o}\right)\right)\right] \tag{8}$$

where C_o' and C_1' have absorbed the normalization and the film transmittance characteristics. With the same paraxial approximation used as before

$$\begin{aligned} s_2 &= [z_1^2 + (x_1 - x_2)^2 + (y_1 - y_2)^2]^{\frac{1}{2}} \\ &= z_1 + \frac{1}{2z_1}\left[r_1^2 + r_2^2 - 2r_1 r_2 \cos(\theta - \phi)\right] \end{aligned} \tag{9}$$

These approximations also allow using $\cos(\hat{n}, \bar{s}) \cong 1$. Changing to polar coordinates and using the integral definition of the Bessel function, one obtains

$$2\pi J_o(a) = \int_o^{2\pi} e^{-ia \cos(\theta - \phi)}\, d\theta \tag{10}$$

then approximating that $s_2 = z_1$, for the denominator of Green's function,

$$U_R = -\frac{i}{\lambda_2 z_1} e^{ik_2 r_2^2/2z_1} \int_o^R U_H J_o\left(\frac{k_2 r_2 r_1}{z_1}\right) e^{ik_2\left(r_1^2/2z_1\right)} r_1 dr_1 \tag{11}$$

R is the maximum aperture determined by the size of the hologram or by the amplitude sensitivity of the film emulsion. The integration limits can be made constant by using the change of variable $r_1 = Rw$; then

$$U_R = -\frac{iR^2}{\lambda_2 z_1} e^{-ik_2 r_2^2/2z_1} \int_0^1 U_H(w) J_o\left(\frac{k_2 r_2 R}{z_1} w\right) e^{i(k_2 R/2z_1)w^2} wdw \tag{12}$$

After expanding the cosine term of U_H the reconstruction amplitude can be written as

$$U_R = \sum_{j=1}^{3} K_j \int_0^1 J_o(vw)\, e^{iu_j w^2} wdw \tag{13}$$

where

$$v = \frac{k_2 r_2 R}{z_1}$$

and

$$\left.\begin{aligned}
u_1 &= \frac{k_2 R^2}{2z_o} & K_1 &= -\frac{iR^2}{\lambda_2 z_1} C_o B' e^{ikr_2^2/2z_1} \\
u_2 &= \pi R^2 \left(\frac{1}{\lambda_1 z_o} + \frac{1}{\lambda_2 z_1}\right) & K_2 &= -\frac{iR^2}{\lambda_2 z_1} C_1 B' e^{ik_1 z_o} e^{ikr_2^2/2z_1} \\
u_3 &= \pi R^2 \left(\frac{1}{\lambda_1 z_o} - \frac{1}{\lambda_2 z_1}\right) & K_3 &= -\frac{iR^2}{\lambda_2 z_1} C_1 B' e^{-ik_1 z_o} e^{ikr_2^2/2z_1}
\end{aligned}\right\} \tag{14}$$

The three integrals are successively the reconstruction caused by a d-c bias on the film, the virtual image, and the real image. Following from the recording geometry described in Fig. 1., all three images overlap. The spatial separation of the images obtained with an off-axis (side band) holographic system would change the details but not the general form of the reconstruction integral. Therefore, the integral contains the salient features of a point source reconstruction.

3.0 RECONSTRUCTION CHARACTERISTICS

The solution of the integral of the form

$$V = \int_o^1 J_o(vw)\, e^{iuw^2}\, wdw \tag{15}$$

can be made using Lommel functions (Ref. 5). The intensity obtained from VV* can be graphically represented by a set of isophote diagrams (Refs. 5 and 6) in which contour lines of equal intensity near the focus of the optical system are plotted on a (u, v) coordinate system. The importance of these isophote diagrams is that the Eq. (15) solution they represent was worked out in analyzing the three-dimensional light distribution near the focus of a diffraction-limited lens. In other words, the intensity field in the focused region of the reconstruction of the hologram of a point source is identically the same as the intensity field near the focal volume of a diffraction limited lens. Thus, the focusing characteristics of the lens apply equally well to the holographic reconstruction. In particular,

1. The fraction of the total energy which falls within a given area about the optical axis for any constant u is the same for point images obtained by lens projection and holographic reconstruction (where the reconstructed images are separated);
2. The phase distribution near focus is the same in both cases, i. e., in the focal waist the phase surfaces propagate like plane waves.

Two special solutions to Eq. (15) are available. When the focus condition is satisfied, $\lambda_2 z_1 = \pm\lambda_1 z_o$ (the +(-) is for the real (virtual) image) then u = o and

$$U = \int_o^1 J_o(vw)wdw = \frac{J_1(v)}{v} \tag{16}$$

The resulting intensity (normalized to unity at the focal center) becomes

$$I_{u=o} = \left[\frac{J_1\left(\frac{k_2 r_2 R}{z_1}\right)}{\frac{k_2 r_2 R}{z_1}}\right]^2 \tag{17}$$

which is the same as the Fraunhofer diffraction from a circular aperture of radius R. Analogously, the hologram behaves like a lens of radius R with a focal distance z.

The second special solution is obtained when $r_2 = o$ which is satisfied along the optical axis. Then $v = o$ and

$$U = \int_o^1 e^{iuw^2} \, wdw = \frac{i}{2u}\left(e^{iu} - 1\right) \tag{18}$$

and the normalized intensity becomes

$$I_{r_2=0} = \text{sinc}^2\left[\frac{\pi R^2}{2}\left(\frac{1}{\lambda_1 z_o} \pm \frac{1}{\lambda_2 z_1}\right)\right] \tag{19}$$

where $\text{sinc}(\alpha) = \sin(\alpha)/\alpha$ and the +(-) represents the virtual (real) image. This intensity distribution can be considered as a focal depth spread function of a point image. In other words, it gives the intensities at points a small distance, Δz, away from the true focus position. Consider

$$\lambda_1 z_o = \pm \lambda_2 z_1 + \lambda_2 \frac{\Delta z}{2} \tag{20}$$

then approximately

$$I_{r_2=0} = \text{sinc}^2\left[\frac{\pi R^2 \Delta z}{4\lambda_2 z_1^2}\right] \tag{21}$$

The out-of-focus distance is $\Delta z/2$. The focal depth can be considered to be the distance Δz from out-of-focus position $(-\Delta z/2)$ to out-of-focus position $(+\Delta z/2)$ such that the intensity does not drop below a given part p of the maximum (at $\Delta z = 0$). Usually a 20-percent reduction from the maximum intensity (i.e., $p = 0.2$) is allowed (Ref. 5). By expanding the sine function and using the first two terms, it follows that

$$\Delta z = \lambda_2 \left(\frac{z_1}{R}\right)^2 \frac{4}{\pi}\left[6(1 - \sqrt{1 - p})\right]^{1/2} \tag{22}$$

The spread between the 80-percent intensity points on either side of focus is

$$\Delta z \cong \lambda_2 \left(\frac{z_1}{R}\right)^2 \tag{23}$$

The lens analogy is that the focal depth of the lens increases with the f-number, represented by z_1/R.

4.0 FOCAL DEPTH EXPERIMENT

The effectiveness of Eq. (23) was tested experimentally. An object field of equally spaced 100-μ -diam wires was made. The object is pictorially like a ladder in which the wires serve as rungs. The wire spacing was 3.048 ± 0.008 cm. The wires were positioned in a 5-cm collimated He-Ne laser beam such that the longitudinal axis of the "ladder" was displaced from the illumination propagation direction sufficiently that all the wires were illuminated. The effective spacing between the wires along the direction of the beam propagation was 3.043 ± 0.008 cm. Holograms were made using Agfa 10E75 film. The distance from the nearest wire relative to the film plane was 32 cm. Reconstruction was by a collimated He-Ne laser beam. In the reconstruction the distances between successive wire images (judged to be at their best focus) were measured. By averaging and calculating the standard deviation, the distance between the reconstructed images was found to be 3.04 ± 0.15 cm. From multiple repetition of the experiment, the standard deviation was found to vary by about ±0.03 cm. In correlating the separation distance with the uncertainty of the focal position of each reconstructed wire image it was assumed that each wire contributes an equal amount to the uncertainty of the distance between the wire image. Then the image position uncertainty is one half the uncertainty of the separation distance. Thus, the focused image is located with an uncertainty of one half the above standard deviation; in other words, $\Delta z = (0.15 \pm 0.03)$ cm. It should be emphasized that this is an average from many data points; it is not intended to imply that each wire reconstruction can be focused satisfactorily within such a tolerance. Rather, the average result implies that any particular focused image location cannot be measured with greater accuracy.

Equation (23) cannot be applied directly to finding the theoretical image position spread for this experiment because z varies for each wire. However, analogously to the experimental averaging procedure, one can find an average Δz spread due to all the wire images. When R is considered a constant, the averaging procedure is facilitated by letting

$$z_1 = z + md \tag{24}$$

The term z is the distance from the film plane to the nearest wire (32 cm), d is the spacing between wires (3.043 cm), and m ranges from zero to N the total number of wires in the object field. An average $\overline{\Delta z}$ for the 80% intensity envelope case is obtained from

$$\begin{aligned}\overline{\Delta z} &= \frac{1}{N}\sum_{m=o}^{N-1} \Delta z_n \\ &= \frac{1}{N}\frac{\lambda_2}{R^2}\sum_{m=o}^{N-1}(z + nd)^2 \\ &= \frac{\lambda}{R^2}\left[z^2 + zd(N-1) + \frac{1}{6}d^2(N-1)(2N-1)\right]\end{aligned} \tag{25}$$

There remains the problem of determining an effective aperture radius R of the hologram. This parameter is usually described in terms of the resolution characteristics of the film used, the assumption being that oscillations in the diffraction pattern are recorded up to the limit of the number of lines per millimeter which the film can resolve. It is easy to show that this assumption does not satisfactorily relate to the problem at hand. Consider the diffraction from a single wire. The oscillatory part of the intensity varies as

$$I \sim \frac{\sqrt{\lambda_1 z_o}}{x_1} \sin\left(\frac{k_1 a x_1}{z_o}\right) \sin\left(\frac{k_1 x_1^2}{2 z_o} + \frac{\pi}{4}\right) \tag{26}$$

where a is the wire cross-sectional radius and the other parameters are as defined before. The sine term with the linear x_1 argument serves as an envelope to the other more rapidly oscillating sine term. It can be shown that if a film has a resolution given as n lines per millimeter, the x_1 distance in centimeters for which this limit is reached by the wire diffraction is

$$x_1 = 10 n \lambda_1 z_o \tag{27}$$

For typical parameters: $\lambda_1 = 0.6328\mu$ (He-Ne laser), n = 2000 (Agfa Gaevert 10E75), $z_o = 5$ cm; then $x_1 = 63.3$ cm. Obviously, this far exceeds the size of film plates. Furthermore, the paraxial approximations are so thoroughly violated that the accuracies of Eqs. (23 and 26) are very questionable.

The effective aperture radius, R, could in principle be determined by knowing the dynamic range of the film and then calculating the smallest visibility which could be recorded. This information was not available and consequently a more direct, although less rigorous, approach was used. The intensities of the diffraction pattern of the hologram of a single wire were obtained by scanning the hologram with a microdensitometer. It was found that the oscillatory information trace could not be distinguished from random variations past approximately the fourth minimum of the linear argument sine term. This corresponds to a distance from the center of the diffraction pattern of

$$x_1 = \frac{2\lambda_1 z_o}{a} \tag{28}$$

This distance is equated to R. It may appear that R should be equal to $2x_1$; this is not the case because it may be shown from the mathematics of the reconstruction of the wire hologram that the diffraction on each side of the center of the pattern contributes only to the reconstruction of the edge of the respective side of the wire. It is as though the hologram were made of two holograms, each reconstructing half of the wire image.

When the reconstruction is in focus $z_o = z_1$ and

$$R = \frac{2\lambda_1 z_1}{a} \tag{29}$$

Substituting Eq. (29) into Eq. (23), z_1 now appears in both the numerator and denominator, therefore cancelling, and the averaging processing of Eq. (25) is no longer necessary. The depth of field becomes simply

$$\Delta z = \frac{\lambda_2}{4}\left(\frac{a}{\lambda_1}\right)^2 \tag{30}$$

The depth of focus in dependent only on the wire radius and on a change of wavelength between recording and reconstruction. For the experimental conditions of $\lambda_1 = \lambda_2 = 0.6328\ \mu$ and $a = 50\ \mu$, one obtains $\Delta z = 1.0$ mm. This is satisfyingly close to the (1.5 ± 0.3) mm depth of field observed experimentally.

The above manner of obtaining the effective film aperture, R, rests on judgmental criterion (i.e., visual interpretation of the microdensitometer trace) rather than more definitive characteristics based on film response and development effects. In that sense the above result should be only cautiously interpreted as a successful experimental verification of the theory. Further measurements of film dynamic range and visibility function are necessary to justify more firmly the above determination of effective film apertures.

An additional interpretational difficulty of the experimental results is that the intensity range of the focal depth was rather arbitrarily chosen for 20-percent variations from the maximum (in focus) value. This value is given by Born and Wolf (Ref. 5) but without any discussion. Different values will, of course, change the theoretical depth of focus as can be seen from Eq. (22).

5.0 SUMMARY

The focused image of the reconstruction of a hologram of a point radiation source is shown to have identically the same intensity and phase characteristics as a point image obtained by a diffraction limited lens. Specifically the reconstructed image has an intensity spread function (Eq. 17) and a focal depth (from Eq. 21), which are the same as for a diffraction limited lens, and within its focal waist the propagation is plane. That the results of the two imaging processes yield identical results is interesting because their focusing phenomena are different, one being a refractive process, the other a diffractive process. The similarity of the results becomes less striking when the diffraction limited lens derivation is examined in its philosophical components. In that derivation it is assumed that perfectly converging coherent spherical waves (produced by the refractive phenomenon) are limited in extent by an aperture. The subsequent results are all due to diffraction by the aperture. Essentially the refractive phenomenon is not really an integral part of the derivation. Nevertheless, its results have been well born out by experimental studies (Ref. 7) and its acceptance is universal.

An experiment was performed to test the focal depth of the reconstructed image. The theoretical predictions were observed experimentally within the cautions of using interpretational data. These results show that depth of focus is dependent on the object size. The size of the objects chosen (wires) were designed to simulate typical particle field. To this effect, it is shown that the depth of focus of particles of 50-μ radius cannot be better than about one millimeter.

REFERENCES

1. Yu, Francis T. S. Introduction to Diffraction, Information Processing, and Holography. MIT Press, Cambridge, Mass., 1973.

2. Goodman, Joseph W. Introduction to Fourier Optics. McGraw-Hill Physical and Quantum Electronics Series, McGraw-Hill Book Co., San Francisco, 1968.

3. Jackson, John David. Classical Electrodynamics. John Wiley and Sons, Inc., New York, 1962.

4. DeVelis, John B. and Reynolds, George O. Theory and Applications of Holography. Addison-Wesley Publishing Co., Reading, Mass., Pergamon Press, Oxford, 1965.

5. Born, Max, and Wolf, Emil. Principles of Optics; Electromagnetic Theory of Propagation Interference and Diffraction of Light. Pergamon Press, Oxford, 1965.

6. Linfoot, E. H. and Wolf, E. "Phase Distribution Near Force in an Aberration-Free Diffraction Image." Proc. Phys. Soc. B, Vol. 69, Pt. 8, p. 823, 1956.

7. Taylor, C. A. and Thompson, B. J. "Attempt to Investigate Experimentally the Intensity Distribution Near the Focus in the Error-Free Diffraction Patterns of Circular and Annular Apertures." J. Opt. Soc. Am., Vol. 48, No. 11, p. 844, 1958.